Research Article

Preparation of Polyaniline Emeraldine Salt for Conducting-Polymer-Activated Counter Electrode in Dye Sensitized Solar Cell (DSSC) using Rapid-Mixing Polymerization at Various Temperature

Auliya N. Amalina[1], Veinardi Suendo[1,2]*, Muhammad Reza[1], Phutri Milana[1], Risa R. Sunarya[1,3], Damar R. Adhika[2], Viny V. Tanuwijaya[2]

[1]*Division of Inorganic and Physical Chemistry, Faculty of Mathemathics and Natural Sciences, Institut Teknologi Bandung, Jl. Ganesha No. 10 Bandung 40132, Indonesia.*
[2]*Research Center for Nanoscience and Nanotechnology, Institut Teknologi Bandung, Jl. Ganesha No.10, Bandung 40135, Indonesia.*
[3]*Department of Chemistry Education, Faculty of Tarbiyah and Teacher Training, UIN Sunan Gunung Djati, Jl. A.H Nasution No. 105, Bandung 40614, Indonesia.*

Abstract

Polyaniline Emeraldine Salt (PANI ES) as a conductive polymer has been used as a Pt-free counter electrode materials in DSSC. In this study, polymerization temperature was varied at relatively high temperature from 308 to 348 K with respect to the standard low polymerization temperature at 273 K. The synthesis held in varied high-temperature to study the effect of synthesis condition resulted to the performance as counter electrode in DSSC. The effect of high-temperature synthesis condition gives interesting results, the FTIR-ATR spectra show the presence of vibrational modes of phenazine structure obtained at high polymerization temperature, indicate the changing in the chain geometry. Raman Spectroscopy shows the decrease of the I_{1194}/I_{1623} intensity ratio that can be interpreted that the degree-of-freedom of C–H bond bending mode decreases in the benzenoid ring, while the stretching mode degree-of-freedom along the chain is preserved or increased. The electrical conductivity profile has changed from metal-like at low-temperature into a semiconductor-like profile at high-temperature. Scanning Electron Microscope images reveals that a change in the morphology of PANI ES with temperature. At low-temperature (273 K) the morphology has a globular shape, while at high-temperature it tends to form nanorod structure. DSSC device with highest efficiency is attained for PANI ES polymerized at 273 K (1.91%) due to its high conductivity. The lowest efficiency is observed in device using PANI ES synthesized at 328 K (1.15%) due to its low conductivity due to the formation of phenazine structure. Copyright © 2019 BCREC Group. All rights reserved

1. Introduction

Dye-Sensitized Solar Cell (DSSC) is the third generation of solar cell introduced by Matsumura in 1977 using a mesoporous ZnO semiconductor [1,2]. In principle, DSSC is a photoelectrochemical cell, which firstly developed as an electrochemical solar cell without any sensitizer but using semiconductor that intrinsically absorbs light in visible range, i.e. CdS [3]. Further developments favor application of sensitizers on
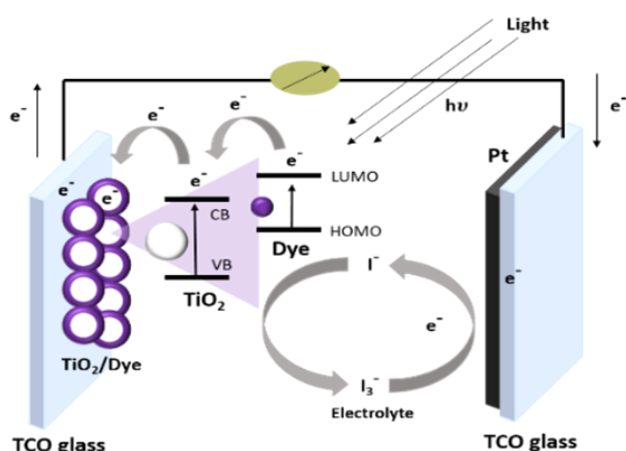
* Corresponding Author.
  E-mail: vsuendo@chem.itb.ac.id (V. Suendo);
  Tel.: +62 222502103. Fax: +62 222504154

mesoporous oxide semiconductors due to their stability and electrocatalytic activities [2-4]. High-efficient TiO_2 based DSSC was firstly developed by O'Regan and Gratzel in 1991 by replacing ZnO with TiO_2 [4]. In DSSC, the electricity was generated from the photoexcited electrons of dye molecules after absorbing light. The electrons from excited states of dye molecules will be injected into TiO_2 conduction band. Injected electrons will flow through the external circuit to the counter electrode producing electric current. The oxidized dye molecule will be regenerated by redox agent in electrolyte, i.e. I_3^-/I^- redox couple [5]. Oxidized redox agent will be reduced back on the surface of counter electrode forming a closed electrical loop. Figure 1 shows the schematic of electrical current generation in DSSC.

DSSC consists of several components, such as photoanode, electrolyte, and counter electrode. Photoanode is made of transparent conductive glass/TCO (e.g. ITO, Indium Tin Oxide or FTO, Fluorine doped Tin Oxide) covered by dye sensitized mesoporous semiconductor (e.g. TiO_2). Counter electrode is an important part in DSSC playing great roles as an electron collector from the external circuit and electrocatalytic interfaces for redox couple regeneration. Counter electrode requires a high conductive substrate laminated by an electrocatalytic active material. Thus, counter electrode is usually made of highly conductive metal with high electrocatalytic activity, notable noble metals from platinum group, i.e. Pt, Pd, Ru, Rh, etc. In recent years, researchers tend to developed Pt-free DSSC due the scarcity of Pt on earth crust and its high price. This leads to the production of DSSC with lower cost, consequently open a wider market. In most cases, Pt was replaced by carbon based materials, i.e. graphite, activated carbon, graphene, etc. [6]. On the other hand, the applications of conductive polymer to enhance the electrocatalytic activity, like polyaniline (PANI), polypyrrole (Ppy), PEDOT/PPS, etc. increases significantly [6].

PANI has some advantages such as easy to synthesize, wide range conductivity, easy doping/de-doping process, and good chemical stability [7,8]. PANI has been frequently used as counter electrode material, notably PANI ES. As counter electrode, PANI ES is usually mixed with graphite to increase its electrical conductivity, while PANI ES provides good electrocatalytic activity. It has been previously reported that PANI ES on flexible graphite counter electrode can produce DSSC with efficiency 7.36 % [9]. To have PANI ES with high conductivity, the polymerization has to be performed at low-temperature [10,11]. However, low-temperature polymerization is generally more difficult to control with respect to the high-temperature polymerization. Previously reported synthesis temperature condition resulted in significantly different electrochemical behavior compared to the low-temperature condition, and high-temperature condition leads to change in the chain geometry [12] The change in the chain geometry can result to the increasing of dielectric constant of the conjugated polymer. High dielectric constant might facilitate better charge transfer and electrocatalytic process in the surface of counter electrode, and there are several reports of high dielectric constant of PANI materials [13-15]. This study focuses on the PANI ES with HCl-doped synthesis using high-temperature rapid-mixing method. High-temperature polymerization means cheaper process, simpler experimental set-up, and more controllable condition than at low-temperature. High-temperature synthesized PANI will be used as the electrocatalytic material for counter electrode in DSSC.

2. Materials and Methods

PANI ES was synthesized at 273, 308, 328, and 348 K in ethylene glycol bath. In a typical procedure, bottle A that contain 3.64 gram (40 mmol) of aniline (Sigma-Aldrich) was dissolved in 100 mL of HCl 1 M (diluted from HCl 37% Merck), and kept in the desired temperature for 1 hour. The solution of oxidizing agent was prepared by dissolved 11.42 gram (50 mmol) of ammonium persulfate (APS) (Merck) in 100 mL of deionized water, which prepared in bottle B and kept in the same desired temperature for 1 hour. The polymerization process was

Figure 1. The schematic of photoelectrochemical processes in DSSC under light illumination.

started by introducing the oxidizing agent solution into aniline HCl solution, rapidly mixed and then kept in the desired polymerization temperature. The polymerization process was let to continue until 24 hours to ensure that all aniline monomer were converted into PANI ES. Resulted PANI ES samples was collected through filtration using filter paper on Büchner funnel, followed by washing with HCl 1M solution and acetone. Washing process will be repeated several times until sample free of oligomers. Obtained PANI ES samples were then dried in vacuum oven at ambient temperature.

Fabrication of DSSC consists of photoanode, electrolyte and counter electrode. Photoanode were prepared by screen printing TiO_2 paste with methyl cellulose (TiO_2 from Qingdao Roadsun Titanos Ind Co., Ltd and methyl cellulose from Sigma-Aldrich) on ITO (Zhuhai Kaivo) surface then dried on hot plate at 120 ºC for 15 minutes. The obtained TiO_2 film were sintered in a muffle furnace at 500 ºC for 1 hour. The sintered TiO_2 film then immersed in a N719 (Synthex Technology) dye solution with concentration of 5×10^{-4} M for 20 hours and then rinsed with isopropyl alcohol. Rinsed TiO_2 film

annealed at 80 ºC prior any cell fabrication. Electrolyte solution were prepared by dissolved KI, I_2 and 4-pyridinecarboxylic acid hydrazide (Merck) in acetonitrile (Merck). Counter electrode were prepared by laminating the synthetic graphite film onto glass substrate, then screen-prints the PANI ES/graphite (1:3) in methyl cellulose paste (graphite from Sigma-Aldrich) onto synthetic graphite surface. Resulting films then dried on a hot plate at 120 ºC for 15 minutes. Electrolyte solution is applied dropwise into a sealing-well on photoanode then sandwiched photoanode and counter electrode using two paper clips prior any DSSC performance measurements.

PANI samples were then characterized by Scanning Electron Microscope using a Hitachi SEM SU3500 with EDAX EDS system, a Bruker Alpha FTIR-ATR spectrometer, a Bruker Senterra Raman spectrometer, an Agilent EA4980A precision LCR meter. An ORIEL S013A solar simulator equipped with a Keithley 2400 source meter was used to measure the DSSC performance of all photovoltaic cells.

3. Results and Discussion

Resulting product of high temperature synthesized PANI ES is greenish powder as shown in inset of Figure 2a. The greenish colour is a typical characteristic of PANI-ES (emeraldine salt) that half-oxidized and electrically conductive [16]. FTIR-ATR spectra in Figure 2b confirm that synthesized PANI samples are emeraldine salt by the presence of quinonoid ring (Q) and benzenoid ring (B) vibrational peaks at
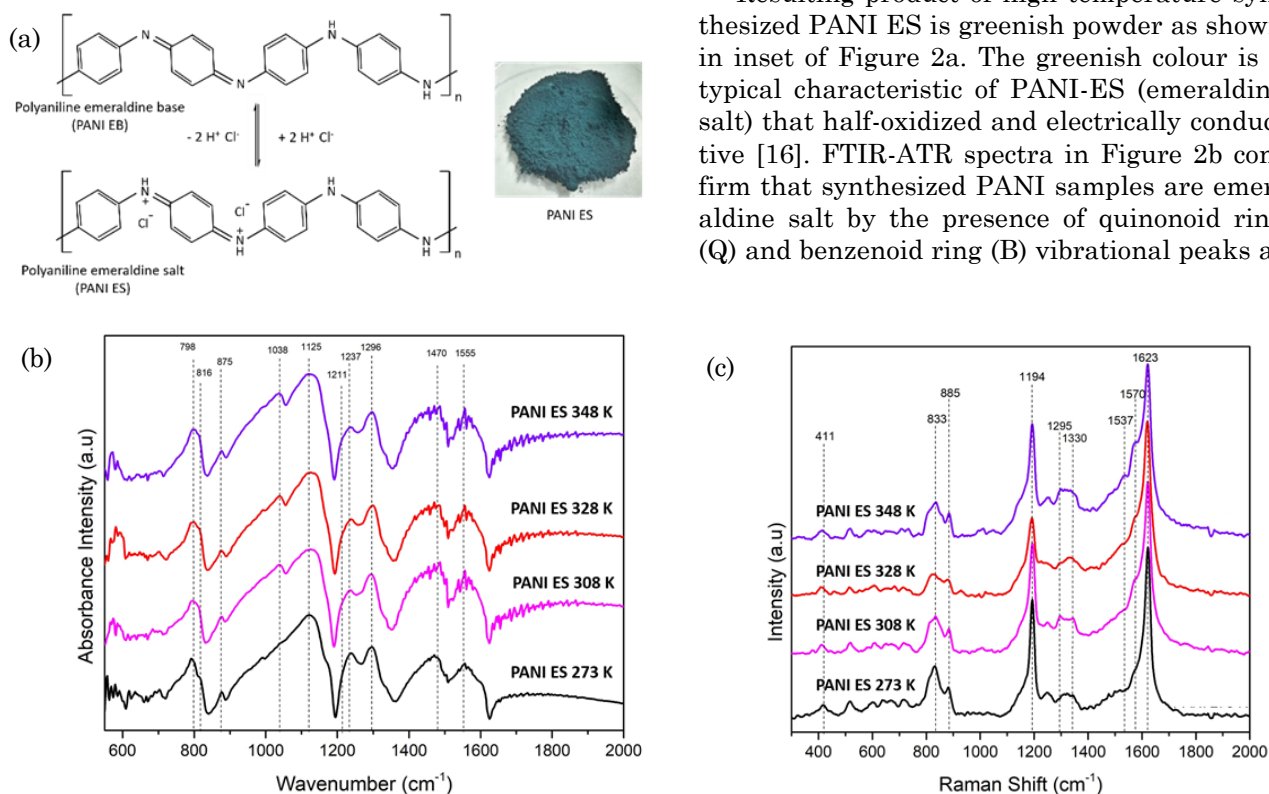

Figure 2. (a) The protonated-deprotonated process of Polyaniline Emeraldine Salt (PANI ES) to Polyaniline Emeraldine Base (PANI EB) and otherwise, the inset image shown green color powder indicating synthesized PANI half-oxidized and well protonated to form PANI ES. (b) FTIR-ATR spectra of PANI ES. (c) Raman spectra of PANI ES excited with 488 nm laser.

1555 cm^{-1} and 1470 cm^{-1}, respectively. The data shows that the peak intensity ratio of Q and B rings vibrational modes (**I$_Q$/I$_B$**) are similar, and indicating the synthesized PANI ES samples are in the half-oxidized state [17]. FTIR-ATR spectra also shown the appearance of new peaks at 1038, 1211, and 1410 cm^{-1} from high-temperature synthesis PANI ES with respect to PANI ES synthesized at 273 K. The peak at 1038 cm^{-1} represents the vibrational modes of phenazine structure. The peak at 1211 cm^{-1} represents the stretching mode of C–N or bending mode of C–H in 1,4-disubtituted or represent the formation of phenazine structure, while the peak at 1410 cm^{-1} represents the combination of vibrational modes from phenazine, safranine, and phenoxazine [18] The phenazine structure was formed due to the fast polymeri-

zation process as a result of high-temperature condition, where anilinium ions created bonds with imine at *ortho* position and then formed phenazine structure.

Raman spectra of PANI ES in Figure 2c shows interesting features, where the peak intensity ratio of **I$_{1194}$/I$_{1623}$** decreases with temperature. The peak at 1623 cm^{-1} represents stretching modes of C=C in benzenoid ring, while the peak at 1194 cm^{-1} represents the C-H bending modes of benzenoid ring [11]. Thus, the **I$_{1194}$/I$_{1623}$** ratio might represent the compactness of polymer chain packing or the degree of freedom ratio between interchain motion and along the chain. The **I$_{1194}$/I$_{1623}$** intensity ratio reaches its minimum at PANI ES 328 K. The decrease **I$_{1194}$/I$_{1623}$** intensity ratio can be interpreted that the degree of freedom of C-H bond bending vibration in benzenoid ring decreases, while the stretching motion degree of freedom along the chain is preserved or increased. This condition can be achieved either by a very compact interchain packing of polyaniline chains or the presence of stiff phenazine structure. The formation of phenazine creates a non-linear PANI ES chain structure, where the carbon atom at *ortho* position of benzenoid ring form a bond with nitrogen atom.
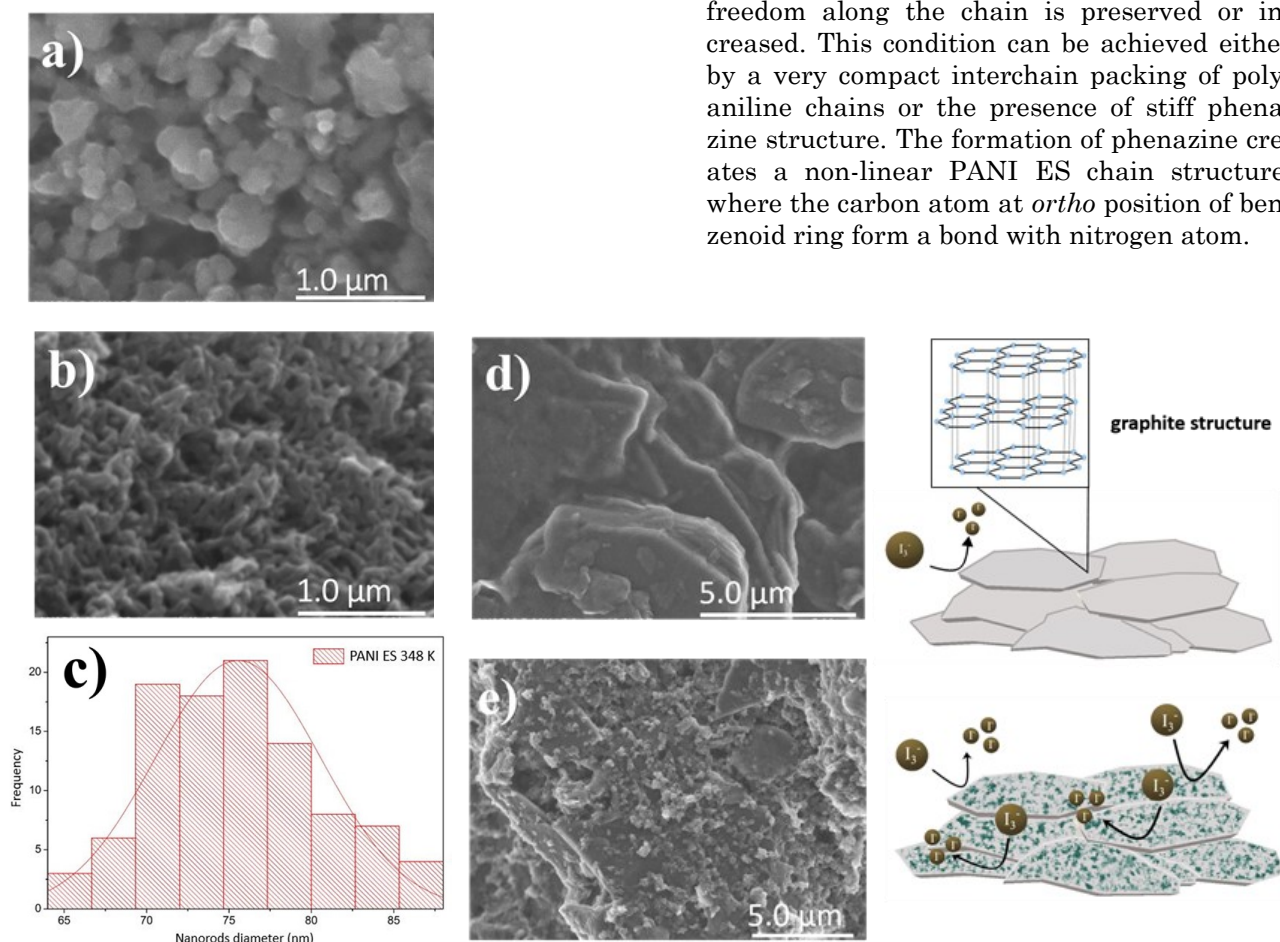

Figure 3. SEM images of synthesized PANI ES at 237 K resulting particles globular morphology (a), and at 348 K resulting particles with nanorod morphology (b). Nanorod particles in (b) show a one modal diameter distribution centered around 75 nm (c). SEM image of graphite counter electrode surface and the inset shows the schematic of electrocatalytic process on the edge of basal plane structure of graphite (d). SEM image of graphite/PANI ES blend counter electrode showing the small PANI ES particles on the surface of graphite plates, where its electrocatalytic process is facilitated by the presence of PANI ES as depicted in the inset (e).

Morphology of PANI ES samples are shown in Figure 3. Globular shape particles were observed at low-temperature condition, 273 K, while at higher temperature PANI ES samples tend to form nanorods (Figure 3a and 3b). Globular shape is a common and conventional shape of PANI ES synthesized at low-temperature polymerization [19]. It has been reported previously that PANI ES tends to intrinsically form into a nanofibrillar structure, such as: nanofiber and nanorod morphology in polar environment. The diameter of resulted nanorod is from 65 nm to 88 nm as shows the diameter distribution in Figure 3c and centered around 75 nm. Moreover, the polymerization process, polymerization rate, growth-polymers and solvent interfacial tension are also involved to facilitate the formation of nanorod morphology [20].

The high-temperature creates a polymerization condition where the interfacial tension decreases with temperature. It can be expected to form PANI ES in nanorod morphology. The in-terfacial tension between PANI ES and solvent decreases with temperature. It has been reported that the surface tension of water decreases from 75.64 to 62.67 mN/m when temperature increases from 273 to 353 K [21]. Furthermore, the increase of temperature also increases the polymerization rate and may not allow enough time for the polymer chains to coagulate and form globular morphology.

PANI ES samples were used as counter electrode in DSSC in the blend form with graphite. The graphite/PANI ES blend forms an interesting mixture, where PANI ES will covered the surface of graphite basal plane structure (Figure 3d). The electrocatalytic process in graphite occurs on the edge of basal plane structure of graphite [22]. Here, the presence of PANI ES that covered the surface of graphite basal plane facilitates more electrocatalytic active sites. High electrocatalytic surface/interface enhances the couple redox regeneration process, i.e. reduces back I_3^- to $3I^-$ as
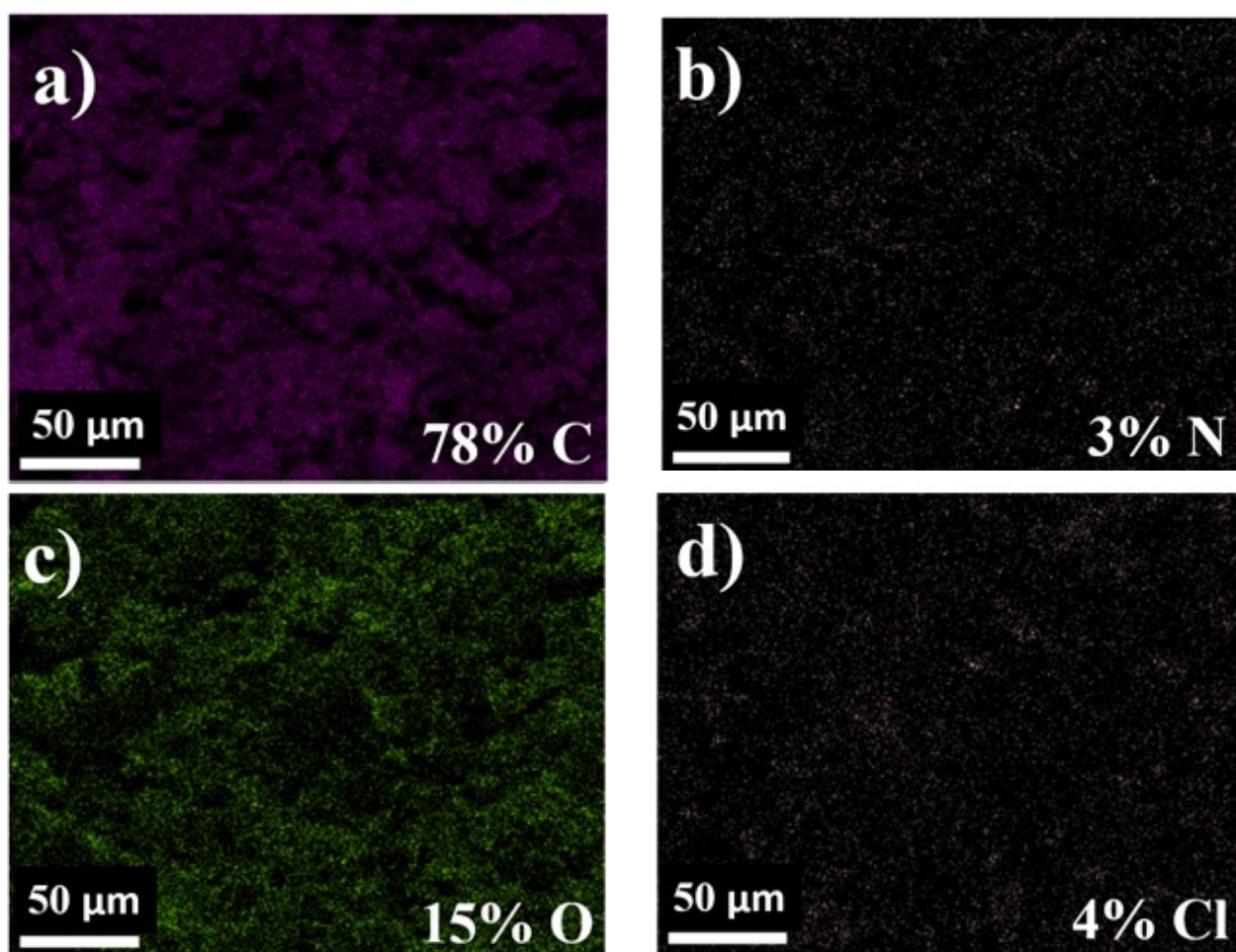
Figure 4. EDX mapping images show the elemental distribution of (a) carbon, (b) nitrogen, (c) oxygen, and (d) chlor on the surface of graphite/PANI ES blend counter electrode.

shown schematically in the inset of Figure 3d. Thus, the graphite/PANI ES blend succeeds to increase the performance of DSSC (Table 1).

The elemental distribution on the surface of graphite/PANI ES blend counter electrode was analyzed using EDX mapping (Figure 4). Figure 4a shows most of the elemental distribution on the surface of graphite/PANI ES blend consist of carbon (78 atomic%), which is mainly from carbon in graphite, PANI ES, and methyl cellulose. Figure 4b shows the elemental distribution of nitrogen (3 atomic%) that comes from the nitrogen atom in PANI ES. Figure 4c shows the elemental distribution of oxygen (15 atomic%) that comes from methyl cellulose as a binder in graphite/PANI ES counter electrode. Figure 4d shows the elemental distribution of chlor (4 atomic%) that comes from HCl as a dopant in PANI ES. We can observed in Figure 4b and 4d that both elements are spread evenly with similar distribution on the surface of counter electrode. This suggests that the PANI EB was successfully doped with HCl to form PANI ES. The presence of Cl atoms that distributed homogeneously on the surface of counter electrode representing polarons ($N^{+}\bullet$) might provide the electrocatalytic sites for I_3^- reduction through coulomb interaction.

The I-V curve of DSSC devices and electrical conductivity profile of PANI ES are shown in Figure 5. The I-V curve shows that the value of J_{sc} decreases with polymerization temperature and reaches a minimum at 328 K. However, it increases again at 348 K. The V_{oc} value does not changed significantly with polymerization temperature. The highest efficiency was obtained by PANI ES 273 K (1.91%) due to the high conductivity. It was observed that the efficiency decreases and reaches its minimum at 328 K (1.15%) due to its low conductivity and the formation of phenazine structure. The presence of phenazine structure can either stabilize or trap the charge carriers [23]. The FF value represents the electrocatalytic efficiency, notably in the regeneration process in DSSC. Graphite/PANI ES 328 K blend provides the minimum value of FF, but it is still higher than graphite-only counter electrode. The FF value of PANI ES 348 K significantly affects its efficiency, whereupon the nanorod morphology might improve the electrocatalytic process in counter electrode due to its large surface are and 3D open channel structure.

Another important factor of PANI ES performance as counter electrode in DSSC is its conductivity [24]. It mentioned above that the highest efficiency in this study is obtained by PANI ES 273 K. PANI ES 273 K also provides the highest electrical conductivity. The electrical conductivity frequency response profile of PANI ES 273 K shows a metal-like profile, where the conductivity decreases with frequency. The metal-like profile in frequency response electrical conductivity provides higher performance than materials with semiconductor-like profile. On the other hand, all high-temperature synthesized PANI ES samples show a semiconductor profile.
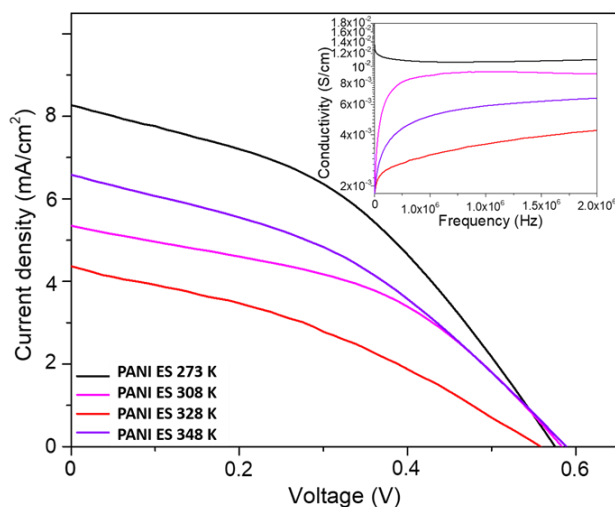
Figure 5. I-V curves of DSSC and the conductivity profile of the materials effects on the devices performance.

Table 1. J_{sc}, V_{oc}, FF, and efficiency of DSSC

Sample	J_{sc} (mA.cm^{-2})	V_{oc} (V)	FF	η (%)
Graphite	7.09	0.59	0.24	1.10
PANI ES 273 K	8.27	0.59	0.41	1.91
PANI ES 308 K	5.35	0.59	0.44	1.34
PANI ES 328 K	4.37	0.56	0.34	1.15
PANI ES 348 K	6.58	0.60	0.38	1.59

4. Conclusions

FTIR-ATR and Raman spectra show the presence of phenazine structure at high-temperature synthesized PANI ES. High-temperature polymerization forms interesting nanorod morphology providing high surface area, despite of the formation of phenazine structure lead to a low electrical conductivity of PANI ES. The increase of polymerization temperature transform PANI ES morphology from globular to nanorods. The performance of PANI ES in DSSC as a counter electrode in the form of graphite/PANI ES blend delivers the highest efficiency with PANI ES 273 K (1.91%). Formation of phenazine structure strongly decrease the DSSC performance as observed in graphite/PANI ES 328 K blend providing the lowest efficiency 1.15%.

Acknowledgement

References

[1]   Tsubomura, H., Matsumura, M., Nomura, Y., Amamiya, T. (1976). Dye sensitized zinc oxide: aqueous electrolyte: platinum photocell. *Nature,* 261: 402-403.

[2]   Matsumura, M., Nomura, Y., Tsubomura, H. (1977). Dye-sensitazion on the Photocurrent at Zinc Oxide Electrode in Aqueous Electrolyte Solution. *Bulletin of the Chemical Society of Japan,* 50: 2533-2537.

[3]   Gerischer, H., Gobrecht, J. (1976). On the Power-Characteristics of Electrochemical Solar Cells. *Berichte der Bunsengesellschaft,* 80(4): 327-338.

[4]   O'Regan, B., Grätzel, M. (1991). A Low-Cost, High-Efficiency Solar Cell Based on Dye-Sensitized Colloidal TiO$_2$ Films. *Nature,* 353: 737–740.

[5]   Ameen, S., Akhtar, M. (2011). Fabrication, Doping and Characterization of Polyaniline and Metal Oxides: Dye Sensitized Solar Cells. *Sol. Cells – Dye. Devices,* 95–130.

[6]   Wu, M., Ma, T. (2014). Recent Progress of Counter Electrode Catalysts in Dye-Sensitized Solar Cells. *J. Phys. Chem. C,* 118: 16727–16742.

[7]   Kulszewicz-bajer, I., Pron, A., Abramowicz, J., Jeandey, C., Oddou, J., Sobczak, J. (1999). Lewis Acid Doped Polyaniline : Preparation and Spectroscopic Characterization. *Chem. Mater.,* 4: 552–556.

[8]   Canales, M., Torras, J., Fabregat, G., Meneguzzi, A. (2014). Polyaniline Emeraldine Salt in the Amorphous Solid State: Polaron versus Bipolaron. *J. Phys. Chem. B,* 118: 11552–11562.

[9]   Sun, H., Lou, Y., Zhang, Y., Li, D., Yu, Z., Li, K., Meng, Q. (2010). In Situ Preparation of a Flexible Poluaniline/Carbon Composite Counter Electrode and Its Application in Dye-Sensitized Solar Cell. *J. Phys. Chem. C.,* 114: 11673-11679.

[10]   Tzamalis, G., Monkman, A., Zaidi, N., Homes, C. (2002). Doping-dependent Studies of the Anderson-Mott Localization in Polyaniline at the Metal-insulator Boundary. *Phys. Rev. B,* 66: 2–9.

[11]   Zhang, L., Wan, M. (2002). Synthesis and Characterization of Self-assembled Polyaniline Nanotubes Doped With D-10- Camphorsulfonic Acid. *Nanotech.,* 13: 750–755.

[12]   Gholamian, M., Contractor, A.Q. (1998). Effect of the Temperature of Synthesis on the Conductivity and Electrochemical Behaviour of Polyaniline. *J. Electroanal. Chem.,* 252: 291-301.

[13]   Brebels, J., Manca, J.V., Lutsen, L., Vanderzande, D., Maes, W. (2017). High Dielectric Constant Conjugated Materials for Organic Photovoltaics. *J. Mater. Chem. A,* 5: 24037-24050.

[14]   Guo, M., Hayakawa, T., Kakimito, M., Goodson, T. (2011). Organic Macro Molecular High Dielectric Constat Materials : Synthesis, Characterization, and Applications. *J. Phys. Chem. B,* 115: 13419-13432.

[15]   Ho, C., Liu, C., Hsieh, C., Hsieh, K., Lee, S. (2008). High Dielectric Constant Polyaniline/Poly(acrylic acid) composites prepared by in situ polymerization. *Synthetic Metals,* 158: 630-637.

[16]   Kolla, H.S., Surwade, S.P., Zhang, X., Macdiarmid, A.G., Manohar, S.K. (2005). Absolute Molecular Weight of Polyaniline. *Communication,* 127: 16770–16771.

[17]   Gomes, E.C., Oliveira, M.A.S. (2012) Chemical Polymerization of Aniline in Hydrochloric Acid (HCl) and Formic Acid (HCOOH) Media. Differences Between the Two Synthesized Polyanilines. *Am. J. Polym. Sci.* 2: 5–13.

[18] Ciric-Marjanovic, G., Trchova, M., Stejskal, J. (2008). The Chemical Oxidative Polymerization of Aniline in Water: Raman Spectroscopy. *Journal of Raman Spectroscopy*, 39: 1375-1387.

[19] Skotheim, T.A., Reynolds, J.R. (2007). *Handbook of Conducting Polymers, Conjugated Polymers Processing and Applications*. CRC Press.

[20] Park, H., Kim, T., Huh, J., Kang, M., Lee, J. E., Yoon, H. (2012). Anisotropic Growth Control of Polyaniline Nanostructures and Their Morphology-Dependent Electrochemical Characteristics. *ACS Nano,* 6: 7624–7633.

[21] Lide, D.R., Baysinger, G., Berger, L.I., Goldberg, R.N., Kehiaian, H.V., Kuchitsu, K., Rosenblatt, G., Roth, D.L., Zwillinger, D. (2005). *CRC Handbook of Chemistry and Physics*. CRC Press.

[22] Yuan, W., Zhou, Y., Li, Y., Li, C., Peng, H., Zhang, J., Liu, Z., Dai, L., Shi, G. (2013). The Edge- and Basal-Plane-Specific Electrochemistry of a Single-Layer Graphene Sheet. *Sci. Rep.*, 3: 1-7.

[23] Kellenberger, A., Dmitrieva, E., Dunsch, L. (2011). The stanilization of charge states at phenazine-like units in polyaniline under p-doping: an in situ ATR-FTIR spectroelectrochemical study. *Physical Chemistry Chemical Physics,* 13**:** 3411-3420.

[24] Ye, M., Wen, X., Wang, M., Iocozzia, J., Zhang, N., Lin, C., Lin, Z. (2015). Recent Advances in Dye-Sensitized Solar Cells : From Photoanodes, Sensitizers and Electrolytes To Counter Electrodes. *Biochem. Pharmacol.*, 18: 155–162.